The American Association of Petroleum Geologists Bulletin
V. 77, No. 10 (October 1993), P. 1710–1722, 12 Figs., 5 Tables

Regional Microseep Survey of Part of the Productive Wyoming-Utah Thrust Belt[1]

Roger G. Dickinson[2] and Martin D. Matthews[3]

ABSTRACT

A regional microseep survey of a 1280 mi² area of the Wyoming-Utah thrust belt clearly identified anomalously high surface occurrences of light hydrocarbons associated with productive trends that include the Clear Creek, Ryckman Creek, and Whitney Canyon–Carter Creek fields. The ethane-to-propane ratios of these anomalies are very similar to those of the hydrocarbons produced from the associated fields.

Anomalies were identified by individually calculating, for each light hydrocarbon, the percentage of samples within a moving window which were above the median value of the entire survey, and by stacking them to create a composite map. This technique smoothes the spatial information and transforms the data from an unknown distribution into a binomial distribution. This permits statistical tests of significance, which have been substantiated with Monte Carlo simulations. The anomalies are both stronger and spatially more extensive than would be expected on a random basis.

The use of regional microseep data emphasizes the identification of broad areas of interest, rather than the direct identification of drilling locations often associated with surface geochemical surveys. The resulting broad surface patterns must then be combined with available subsurface data to develop probable plays. This technique is one of the few tools that analyze directly for hydrocarbons. It provides the explorationist with unique information to help reduce economic and geologic risk in frontier areas.

[1]Manuscript received, December 16, 1991; revised manuscript received, December 28, 1992; final acceptance, January 28, 1993.

[2]Texaco Exploration and Production Inc., P.O. Box 2100, Denver, Colorado 80237.

[3]Texaco Frontier Exploration Department, 4800 Fournace Place, Bellaire, Texas 77401.

We thank the management of Texaco for permission to publish this study. We also thank L. M. Wilson for his insight, guidance, and encouragement in this study, and S. L. Stone for her gifted help with the figures.

INTRODUCTION

The study area is located in the Wyoming-Utah thrust belt between 41°18', and 41°54'N latitude, and 110°36' and 111°15'W longitude (Figure 1). The survey covered approximately 1280 mi² and consisted of 1890 microseep samples. Microseep samples are a surface geochemical technique consisting of methane, ethane, and propane analysis. These gases along with hydrogen, helium, and nitrogen are considered to be "light gases." The study was conducted to ascertain the potential value of regional microseep surveys to exploration play development.

The visual detection of large surface hydrocarbon seeps (macroseeps) is one of the oldest and most successful hydrocarbon exploration techniques. Large areas of North America and the Middle East were initially successfully explored using macroseeps. The existence of macroseepage is generally taken as direct evidence of subsurface hydrocarbons and is thus used to define a region of interest rather than a prospect location (Link, 1952). This regional evidence is then integrated with geological data and, when available, with geophysical data to identify prospects within the region of the seepage. The extension of this technique to the more subtle surface microseeps, through the use of sophisticated analytical techniques, has resulted in substantial controversy regarding drillable prospect definition. This is in part because light gas studies are typified by rapid spatial variations in magnitude. The processing techniques reported here minimize these variations while emphasizing the regional pattern of seepage. This paper will discuss the use of surface microseep data in regional evaluation, not prospect definition.

The presence of surface seeps (macro or micro) unequivocally documents that hydrocarbons have been generated at depth and have migrated to the surface. Of all the surface exploration techniques, only hydrocarbon seeps give direct evidence of the composition of generated hydrocarbons and the spatial pattern of migration before drilling. Hydrocarbon microseep data is not a primary hydrocarbon prospect tool. Its principal use (like that of macroseeps) should be in regional evaluation.

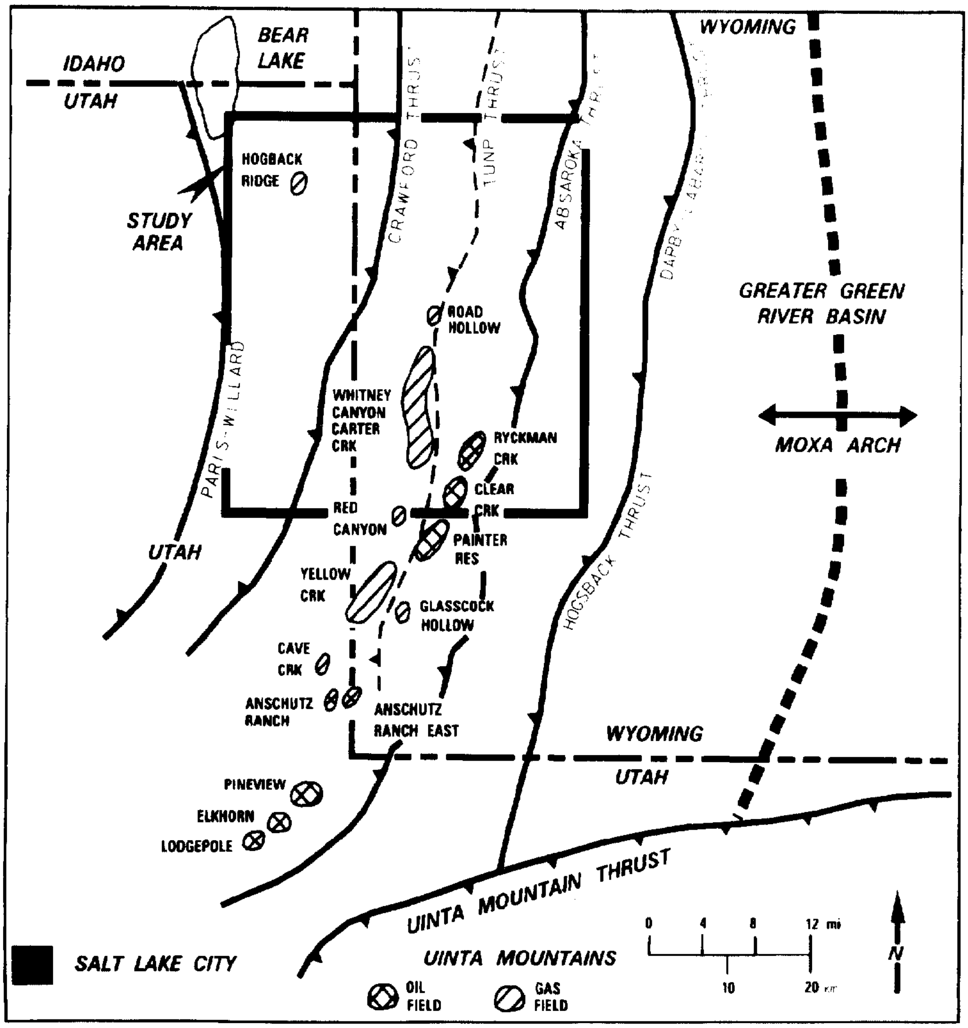

Figure 1—Index map of the study area, showing selective producing fields and significant faults.

PETROLEUM GEOLOGY

Framework

Thousands of feet of predominantly marine sediments (Figure 2) were deposited from the Precambrian to the Devonian on the rifted western edge of the North American continent. This thick accumulation of marine sediments contains significant lateral lithologic and thickness variations.

The western margin of North America has been subjected to periods of subduction and collision with exotic terrains since the Late Devonian. These collisions resulted in episodes of compressive deformation (the Antler and Sonoma orogenies) and the emplacement of exotic terrains onto the North American continent. Important regional structural features initially developed during these episodes of compressive deformation, resulting in changes in deposition during the early Paleozoic (Peterson, 1973, 1977, 1980). Still, in a general sense, upper Paleozoic sediments formed a thick section, as the Cambrian through Devonian sediments had previously done.

Extensive episodes of compressive deformation occurred from the middle Mesozoic through the Tertiary, especially during the Nevada, Sevier, and Laramide orogenies. In the Wyoming-Utah thrust belt from at least the Late Jurassic to the Eocene, major thrusting occurred, primarily associated with the Sevier orogeny. Thrust sheets up to 50 mi wide, 20,000 ft thick, and hundreds of miles long were formed (Dixon, 1982). In general, the early thrusts formed in the west and were later undercut and carried to the east by younger thrusts. This thin-skinned style of thrusting shortened the original sedimentary wedge as much as 50% (Royse et al., 1975). Late Tertiary extensional forces resulted in significant block faulting in the western United States, adding additional structural complexities to the western edge of the thrust belt.

The generalized geology of the survey area

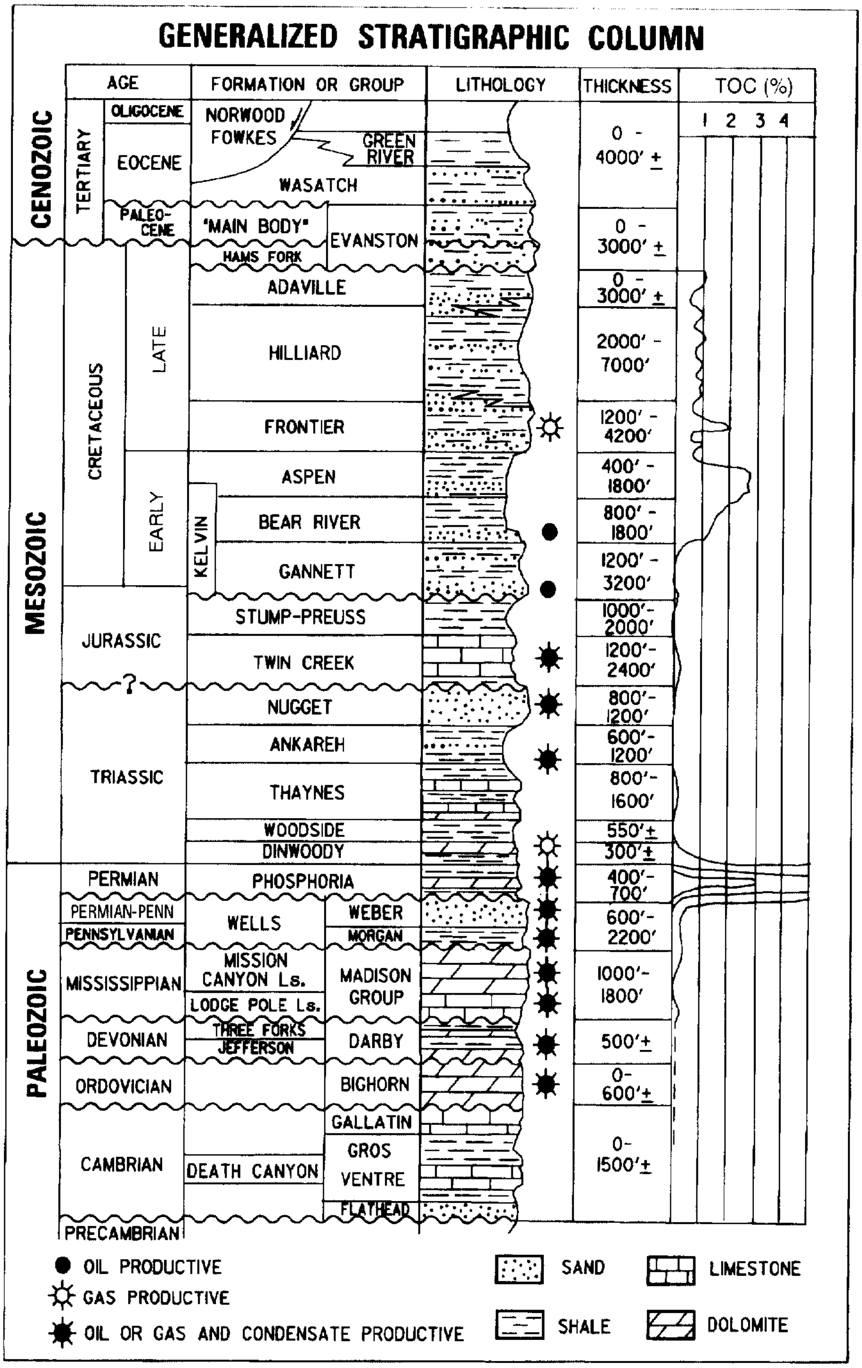

Figure 2—Generalized stratigraphic column showing age and thickness of formations, percent total organic carbon (TOC), general lithology, and productive units (adapted from Lamerson, 1982).

including the surface traces of the Absaroka, Tunp, and Crawford thrusts, is shown in Figure 3. Extensive erosion of topographic highlands during and after thrusting buried Mesozoic and Paleozoic rocks under Tertiary and Quaternary sediments. The extent of faulting and formation of structures in the area is shown in the cross section extending from west of Whitney Canyon-Carter Creek field to east of Ryckman Creek field (Figure 4).

Hydrocarbon Source Rocks

The average total organic carbon (TOC) of formations in the Wyoming-Utah thrust belt is shown in Figure 2. The best potential source rocks are in the Upper and Lower Cretaceous section and possibly in the Permian Phosphoria Formation.

Large sections of Cretaceous sediments have been overridden by thrust sheets in the eastern part of the

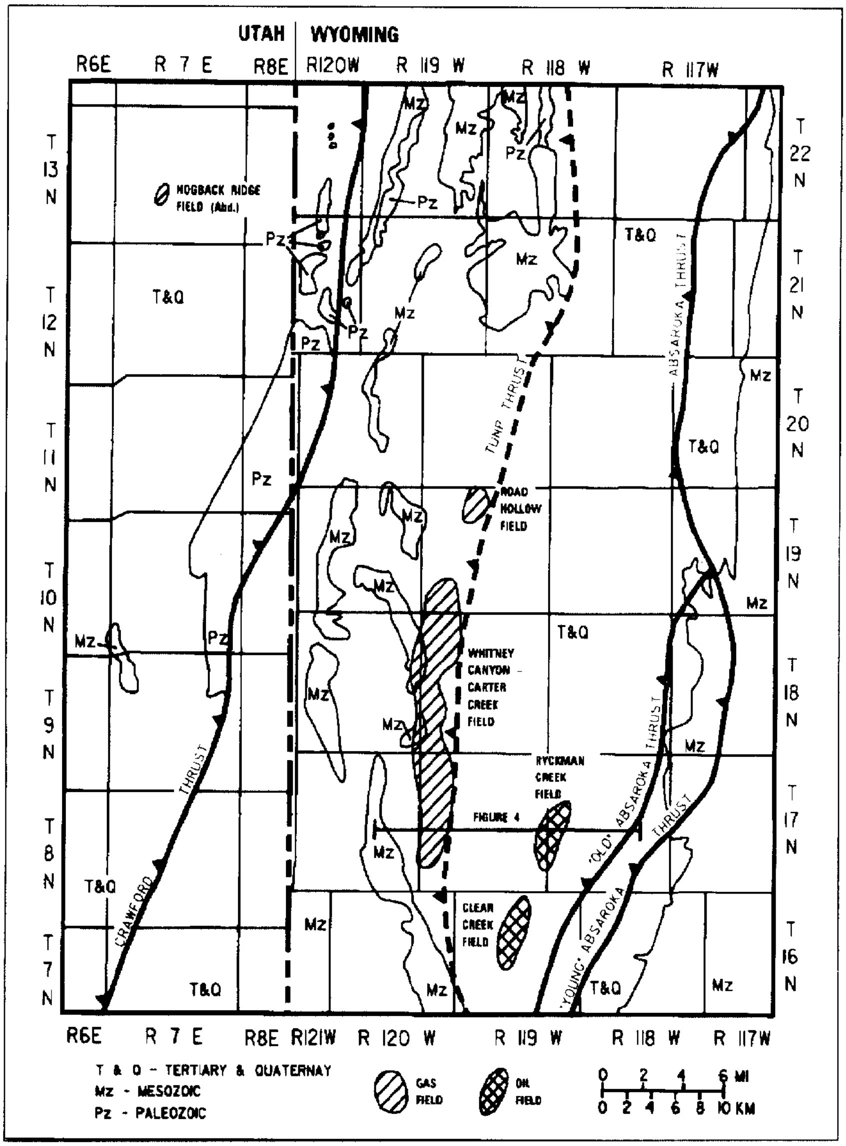

Figure 3—Map showing generalized surface geology of the study area, location of the cross section shown in Figure 4, selective field locations, and type of hydrocarbons produced from each field.

thrust belt. These Cretaceous sediments have generated virtually all of the hydrocarbons within the productive trend of the Wyoming-Utah thrust belt (Warner, 1982). In the vicinity of Ryckman Creek field, Warner (1982) estimated that oil generation in Cretaceous source rocks began shortly after thrusting of the Absaroka fault. Peak generation occurred between 77 and 55 Ma (Late Cretaceous-Paleocene), with oil generation in the Frontier Formation continuing to the present.

Sour gas and condensate production from fields in a westerly line of folding in the thrust belt had initially been attributed to a Phosphoria source. It is now thought that this gas was sourced by more thermally mature Cretaceous shales. The Phosphoria is believed to have been generating hydrocarbons at the beginning of the Sevier orogeny. Pratch (1985) discussed the difficulties in maintaining trap integrity during active thrusting. After thrusting, the Phosphoria was either buried too deeply for any hydrocarbon generation except dry gas, or it was exposed at the surface by erosion. There are no known hydrocarbon accumulations within the study area that were sourced from the Phosphoria.

The preferential migration pathways (stratigraphic and fracture permeability networks) which charged the reservoirs are probably still active and responsible for present-day seepage patterns. One of the reasons that we undertook our survey in the thrust belt was our belief that there would be little true vertical migration and that any geochemical anomalies would act as exploration leads. Development of these leads into prospects would require integration of this data with conventional geologic and geophysical data.

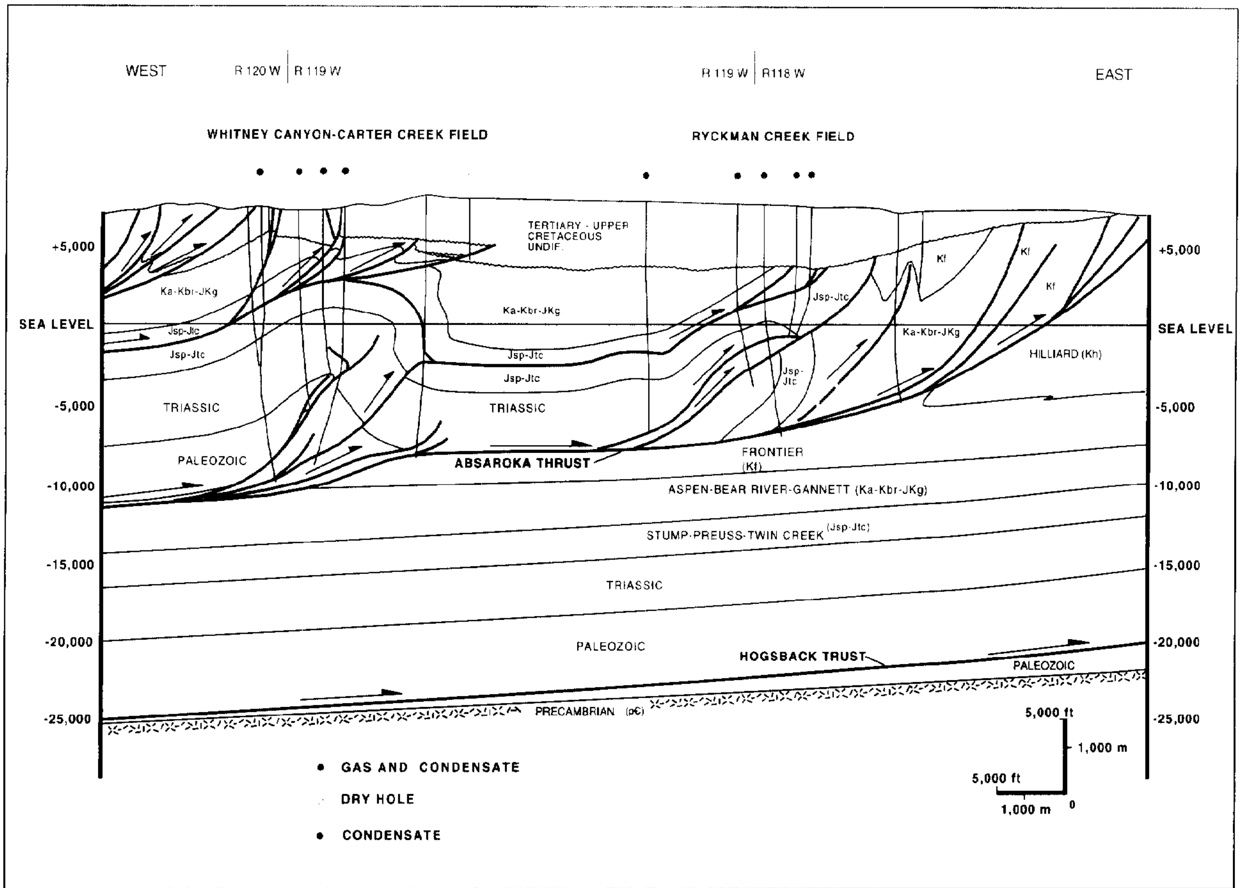

Figure 4—West-east structural cross section through the south part of Whitney Canyon–Carter Creek and Ryckman Creek fields. Line of section is shown in Figure 3. Adapted from Lamerson (1982, his plate 5).

Cretaceous source rocks in the study area are believed to extend no more than a few miles west of the surface trace of the Crawford thrust due to nondeposition, extensive uplift, and erosion (Valenti, 1987). East of the study area, significant amounts of hydrocarbons have been generated from Cretaceous shales between the leading edge of the thrust belt and the Moxa arch. Some of these hydrocarbons have migrated eastward towards the Moxa arch.

Field Production History

Produced hydrocarbons in the thrust belt are contained primarily within two major north-south productive trends (Lamerson, 1982) (Figures 1, 3). The eastern trend produces oil, condensate, and sweet gas; the western trend produces dry to wet gas with condensate. Farther west is Hogback Ridge field, which produced dry gas. This westward decrease in heavy hydrocarbons is the result of a westward increase in thermal maturation of the sub-thrust Lower Cretaceous source rocks.

Analyses of oil, condensate, and light hydrocarbon gases from Ryckman Creek field are shown in Table 1 (Petroleum Information Corporation, 1981). Only the relevant gas components are shown there. The oil gravity value (47.4°) indicates that the liquid is at the oil-condensate boundary. The maximum hydrocarbon column in this field is 515 ft, consisting of 215 ft of liquids and 300 ft of gas. The light hydrocarbon gas in Clear Creek field has an API gravity of 50.1°; Table 1). The hydrocarbon column in this field is composed of 400 ft of gas and 58 ft of liquids. The percentage of produced gas in Clear Creek field is significantly higher than that of Ryckman Creek field.

Five separate productive intervals with gas analyses are shown in Table 1 for Whitney Canyon-Carter Creek field. Variations in the analyses are in response to different amounts of hydrogen sulfide (H_2S) and carbon dioxide (CO_2) that have been introduced locally to the individual productive reservoirs. However, the hydrocarbons appear to have been generated from a single source, most likely Lower Cretaceous shales. The source for the H_2S and CO_2 is believed to be anhydrites within the Upper

Table 1. Gas and Condensate Analysis of Selected Fields in the Study Area

	Ryckman Creek		Clear Creek	Whitney Canyon–Carter Creek					Hogback Ridge
	Nugget Fm.	Thaynes Fm.	Nugget Fm.	Thaynes Fm.	Phosphoria Fm.	Weber Fm.	Madison Fm.	Big Horn Fm.	Dinwoody Fm.
Gas Analysis									
Methane (mol %)	77.86	78.80	79.76	79.50	73.52	57.00	67.16	84.86	84.04
Ethane (mol %)	11.27	10.20	10.77	6.68	8.11	5.82	6.30	6.74	0.44
Propane (mol %)	5.25	5.20	4.71	2.62	2.00	2.02	1.87	2.02	0.02
Hydrogen sulfide (mol %)	nil	0.00	0.00	0.00	6.70	21.34	15.24	0.63	NR
Carbon Dioxide (mol %)	0.05	0.05	0.08	0.10	4.80	5.11	5.75	1.95	0.00
Nitrogen (mol %)	2.31	2.30	2.14	6.51	2.60	1.01	0.60	0.71	15.50
BTU/ft^3	1239	1239	1240	1210	1125	1100	1150	1135	857
Gas/Oil Ratio				48,000:1	57,000:1	48,000:1	51,000:1	55,000:1	
Condensate Analysis									
Gravity (API)	47.4	47.4	50.1						
Sulfur (wt. %)	0.026	0.026	NR						
Hydrogen Sulfide (wt. %)	nil	nil	0.00						
Pour Point (°F)	30.00	30.00	NR						
Viscosity (cp)	1.1	1.1	NR						

NR=not reported.

Mississippian Madison Group. This explains why the percentages of H_2S and CO_2 decrease above and below the Madison Group reservoir.

Estimated in-place reserves for Whitney Canyon-Carter Creek field are 4.5 tcf of gas, 125 million bbl of condensate, and 24 million long tons of sulfur (Sieverding and Royse, 1990). Clear Creek field has estimated reserves of 33 million bbl of liquid hydrocarbons and 200 bcf of gas (Petroleum Information Corporation, 1981). No reliable estimates for Ryckman Creek field are available. By the end of 1991, Ryckman Creek field had produced 193 bcf of gas and 19.2 million bbl of oil (Petroleum Information Corporation, 1991). In addition to these three large fields, there are several small fields within the study area, but gas analysis is available for only the abandoned Hogback Ridge field, Rich County, Utah (Walker, 1982) (Table 1). Hogback Ridge field produced 5.8 bcf of dry gas over a two-and-a-half year period. Nitrogen content of the gas was 15%, with no H_2S or CO_2 present.

Reservoirs within the hanging walls of individual thrust plates are extensively fractured. Of the major productive reservoirs, only the Nugget Sandstone has significant primary porosity (10–12%). Reservoirs in the Twin Creek Limestone, Weber Sandstone, Madison Group, and Big Horn Dolomite are all dependent on fracturing to make them economical. Although the Weber and Madison contain intervals of primary porosity, they are still dependent on fracturing for permeability. Formations such as the Twin Creek (micritic limestone) initially had little primary porosity, and fracturing was critical to its development as a reservoir. Hydrocarbon migration into the reservoirs after thrusting helped to retain existing porosity and permeability.

MICROSEEP SURVEY METHODOLOGY

Locations for the 1890 samples (Figure 5) were selected using topographic maps of the area. Three criteria were used in determining locations: (1) two samples were purposely located in each section (640 ac) to insure an approximately constant sampling density, (2) sample locations were purposely selected adjacent to unusually long and straight stream systems and along the surface traces of the major thrust faults based on the assumption that these features would be related to fracturing and would provide the most effective conduit for any subsurface hydrocarbons present at the surface, and (3) samples were located near roads or other easy access, after the first two criteria were met. Sampling in the field was contracted to Exploration Technologies Inc. (E.T.I.). Because some localities were inaccessible due to unfavorable terrain, difficult access, and permitting problems, there is undersampling in a few areas. Under all conditions, samples were taken at approximately a 4-ft depth using a 4-ft microseep probe. A sampling hole was made manually with a specially constructed 0.5-in. steel bar. A microseep probe was then inserted into the hole, and a gas sample pumped into an evacuated 125-cm^3 serum bottle through a septum. The bottle was then pressurized to about 7 psi over atmospheric pressure to insure that no additional gases would enter the sample container before

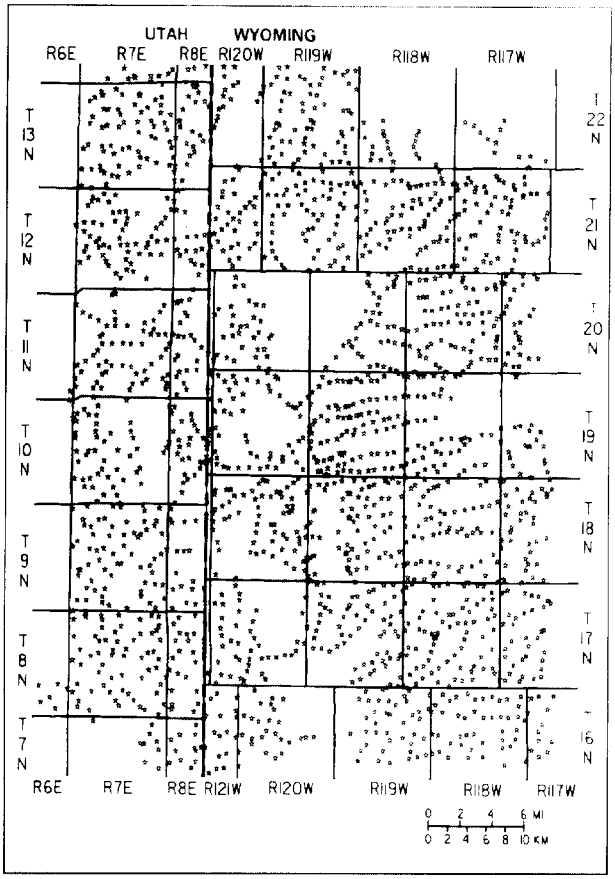

Figure 5—Map of sample locations in the study area. Samples were originally spaced at two per mile. Topography, weather, access, and time constraints did not allow some samples to be collected.

analysis (Matthews et al., 1984). Light gas concentrations were measured by flame ionization gas chromatography, as described in Jones and Drozd (1983). E.T.I. measured and supplied values for methane, ethane, propane, iso-butane, n-butane, ethylene, propylene, helium, and hydrogen for each sample.

Data Manipulation

Surface geochemical data are traditionally interpreted through the use of summary statistical techniques and visual comparison of point-data maps with known geologic features of the area. These mapping techniques focus on the relationship of individual measurements ("trees") to the entire sample population but obscure the regional patterns ("forest"). The interpretive methodology (and sampling density) used in our study specifically focuses on the recognition of these regional trends and their relationships to geologic patterns, at the expense of the fine detail provided by the individual measurements. We intentionally emphasize large regions of preferentially focused hydrocarbon migration. These analysis techniques are also suitable for finer scale studies, provided that the overall sample density is maintained.

The magnitude of surface hydrocarbon concentrations is controlled by (1) subsurface concentration of hydrocarbons in either source rock or reservoir rock, and (2) hydrocarbon migration to the surface as a result of pressure differentials and permeability pathways (Figure 6).

The relationship of surface seepage to permeability pathways, particularly faults and fractures, has been amply demonstrated for macroseeps by Link (1952) and for microseeps by Matthews et al. (1984), Jones and Drozd (1983), and others. The narrowness of these leakage paths is well known in the case of macroseepage, where visual seepage is often confined to very narrow zones and the surrounding rock show only a trace of seepage or none at all. Microseepage shows similar variation, often of more than 2-3 orders of magnitude within 40 ft. This high spatial variability raises concerns about aliasing in sampling programs, particularly at the sparse sam-

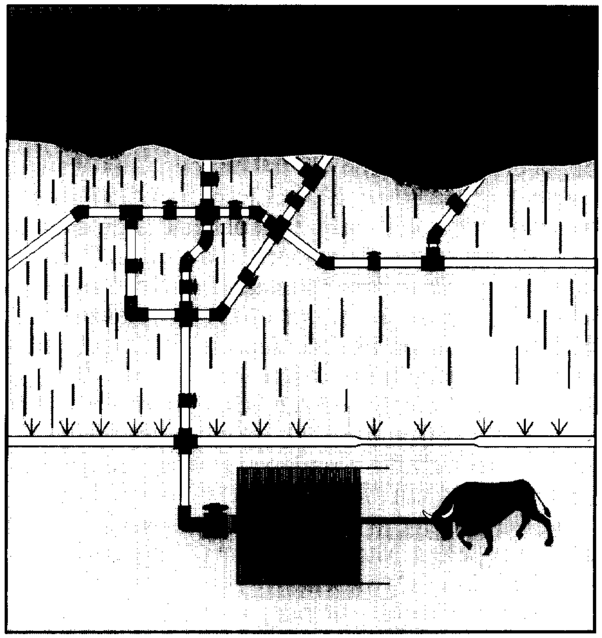

Figure 6—Diagrammatic representation of hydrocarbon seepage. Source rock is represented by the large cylinder at the bottom. Expulsion pressure is represented by the bull. Unfocused leakage from the source rock is represented by the sprinklers. Focused flow and accumulations are represented by the pipes. Valves represent permeability restrictions. The magnitude of hydrocarbon leakage at a surface point is a function of (1) the presence of hydrocarbons in the subsurface, (2) the pressure associated with the hydrocarbons (in the source rock and the reservoir), and (3) the permeability pathway to the surface.

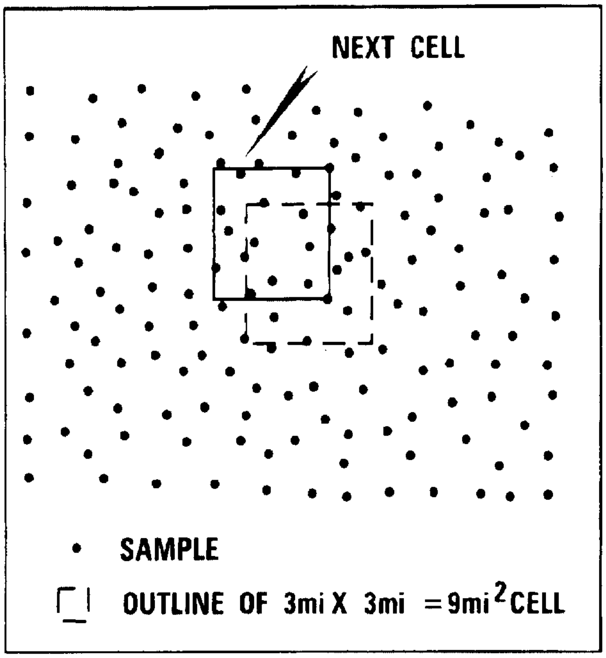

Figure 7—Diagrammatic representation of how the cell is moved across a hypothetical grid of samples. The number of samples within the cell with values greater than the survey median for that gas component are divided by the total number of samples in the cell. The resulting fraction is plotted at the cell center. The cell is then shifted 1 mi, and a new fraction is calculated. This process is continued until the complete sample grid has been covered by cells.

pling density used in this study, and is the reason for the "noisy" character of many surveys.

The statistical technique used in this study was specifically designed to minimize noise and emphasize anomalous regions of high seepage. First the median (50th percentile) value of methane was found for the total sample population. Then a square spatial subsample (cell), 3 mi on each side (9 mi^2) was selected. The number of samples within the cell of magnitude greater than the median methane value of the total population was counted. This number was then divided by the total number of samples in the cell (usually about 18, but as high as 30 and as low as 1) and expressed as a fraction (p), which was given the location coordinates of the cell center. The cell position was then shifted 1 mi and a new fraction was again calculated. This process of cell relocation and calculation was continued in both x and y directions until the entire survey area had been covered (Figure 7). This operation was then repeated for ethane and propane. Maps of these fractions are shown in Figures 8–10. This technique is a variant of kriging, a modified floating average over a standard area, (Davis, 1973), and is similar to the boxcar filtering techniques used in image processing. Maps of these fractions emphasize areas containing a high proportion of samples with hydrocarbons above the population median. These maps identify broad areas where hydrocarbons are migrating through the section and delineate regions where reservoir charging would be most likely. Individual magnitude information is lost, and therefore the exact pattern and magnitude of the flux are not indicated by these maps.

A composite gas value (Figure 11) is generated from the methane, ethane, and propane cell fractions. Stacking the methane, ethane, and propane fractions in this manner further reduces the variation inherent in surface geochemical data and highlights areas where large percentages of all three light gases are above their respective survey medians.

Methane in soil gases can suggest either thermogenic seepage from depth or biogenic generation; isotope composition of the methane is commonly used to differentiate between the two methane sources. However, the presence of appreciable quantities of ethane, propane, and butanes can only be explained by (1) leakage of thermogenic hydrocarbons from depth or (2) contamination.

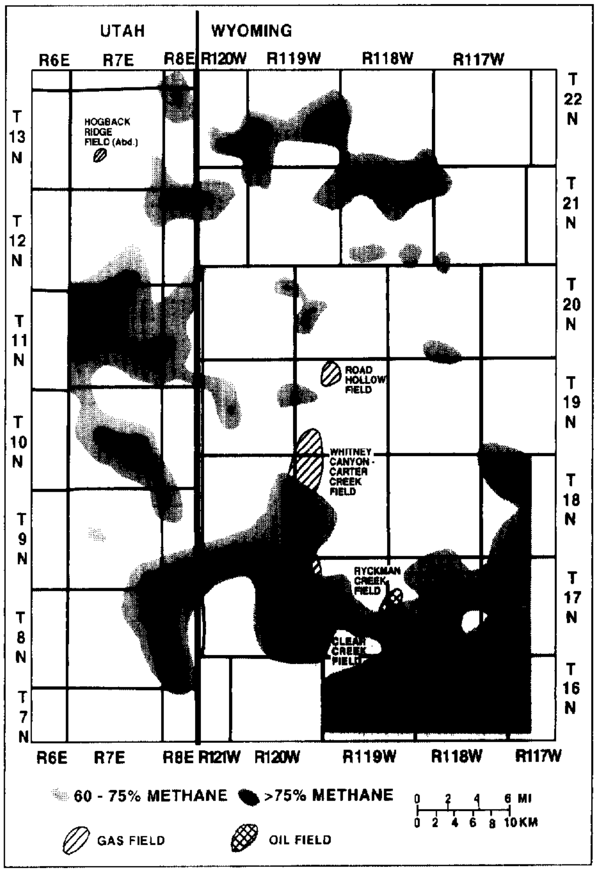

Figure 8—Methane cell map. Areas with high proportions of samples above the median methane concentration are highlighted. Significant fields are indicated.

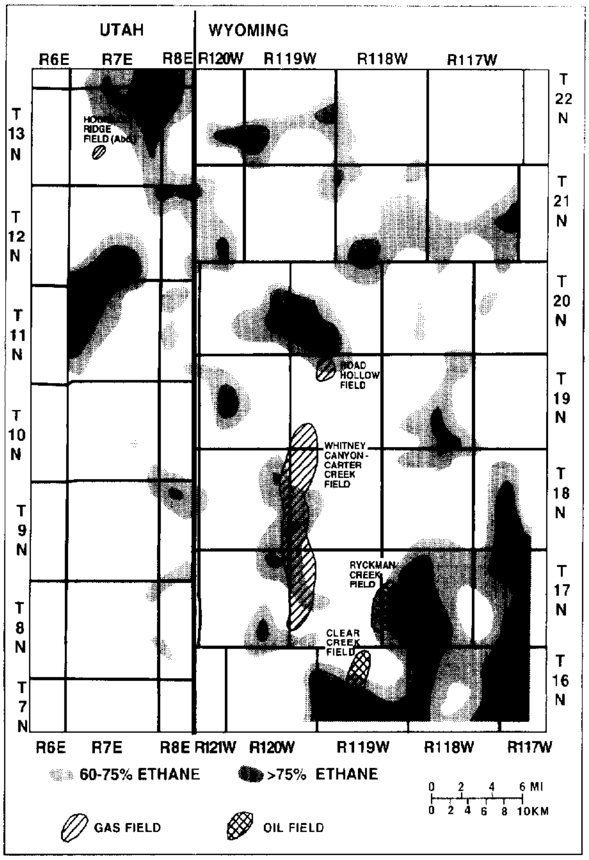

Figure 9—Ethane cell map. Areas with high proportions of samples above the median ethane concentration are highlighted. Significant fields are indicated. Compare areas of concentration with Figures 8 and 10.

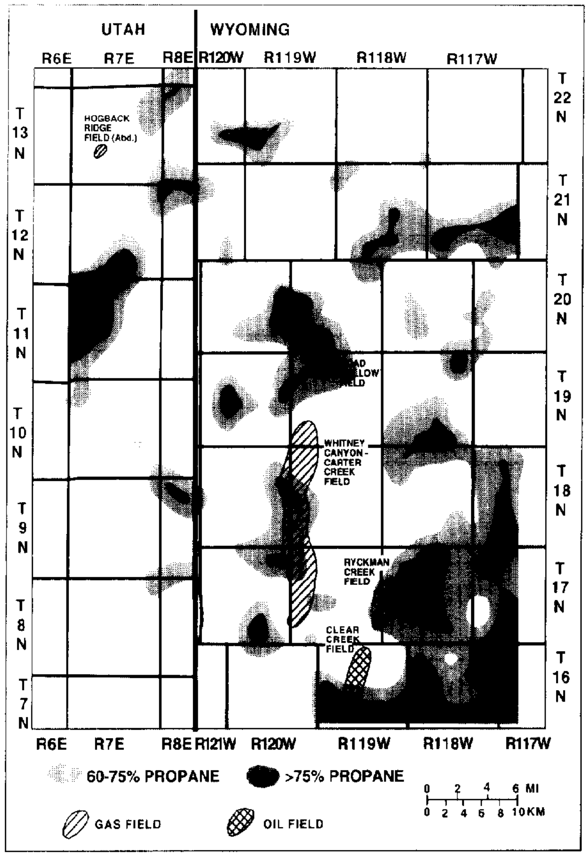

Figure 10—Propane cell map. Areas with high proportions of samples above the median propane concentration are highlighted. The highlighted areas on this map cover similar areas to those on the ethane cell map (Figure 9). Significant fields are indicated.

The probability distribution function for background or unfocused seepage is unknown but is commonly assumed to be either normal or log normal. We avoid this problem by considering each sample as either above or below the median of the sample's population, imposing a binomial distribution onto the entire data set. This has an added advantage: hypothesis test can be determined for anomaly significance. The null hypothesis is that seepage data are random (no spatial focusing). We therefore expect half (0.5) of the samples in each cell to be above the population median and half below. This concept is similar to the expected results of tossing a large number of coins (half heads and half tails). If our null hypothesis is found to be wrong, we can conclude that there is focused hydrocarbon seepage.

Our sampling design (2 samples/mi^2) and cell size (9 mi^2) results in 18 samples per cell, except near the edges of the study area (and in inaccessible areas). Under our null hypothesis (no seepage pattern) and a homogenous binomial distribution with a population (P) equal to 0.5 and n = 18 sampling points for each cell, we expect the observed cell fractions (p) to range between 0.82 and 0.18 (due to natural variation of population estimates) 99% of the time (Dixon and Massey, 1957). Similarly, an observed p value should range between 0.76 and 0.24 all but 5% of the time. This is a two-tailed test, so the expected percentage of fractions in excess of 0.82 and 0.76 are 0.5% and 2.5%, respectively.

The percentage of cells with fractions for methane, ethane, and propane greater than 0.82 and 0.76 above median magnitudes and less than 0.24 and 0.18 below median magnitudes are shown in Table 2. Because we had variations in the spatial density of sampling points, we selected cells with more than 14 samples in them to test the null hypothesis. This gave us some cells with fewer than 18 samples and a larger number of cells with more than 18 samples. The effects of larger and smaller sample size tend to cancel each other out. The values obtained for cells with more than 14 samples in them caused us to reject the null hypothesis of unfocused seepage at both the 1% and 5% level of significance and to conclude that there are areas of focused seepage within the study area. The spatial distribution of seepage is shown in Figures 8–10, 12. For simplicity the maps show only areas of abnormally high spatial concentrations of above median seepage. We have simplified the position of the 0.82 and 0.76 contours to 0.75 because, at this scale, it is difficult to resolve the two contours. We show the position of the 0.60 contour to emphasize a greater region of exploration interest. The exact position of the area of interest should be modified on the basis of geologic extrapolation of the seepage data into the subsurface.

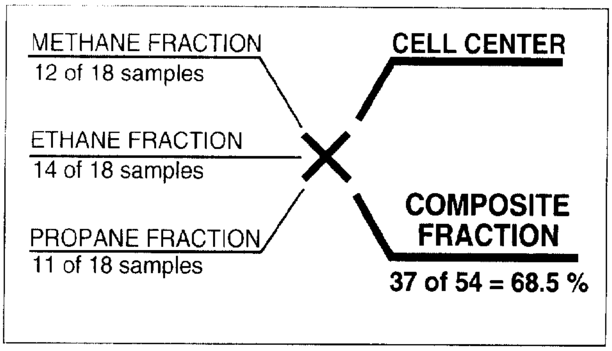

Figure 11—Diagram showing calculation of composite fraction at each cell center. The methane, ethane, and propane fractions are combined to obtain a composite fraction at each cell center.

Statistical Significance of Anomalies

The validity of this processing technique was tested by generating 100 map realizations using Monte Carlo simulations (random, unfocused distribution of high and low values) of the area, using the sample locations. These realizations were processed through the cell programs we have discussed. Scattered anomalies of small to moderate size were observed. The frequency of these anomalies was close to that predicted by the binomial theorem: cells containing more than 14 samples and above median fractions more than 0.76 and less than 0.24 generally covered about 5% of the total area, and cells with fractions more than 0.82 and less than 0.18 generally covered 1% of the area, justifying the use of cells with more than 14 samples to test the null hypothesis. When all cells were counted, the above-median fractions more than 0.76 and less than 0.24 increased to about 8%, and fractions more than 0.82 and less than 0.18 increased to about 4%. In all cases, the abnormally high and low fractions were symmetrical. The increase in anomalous percentage from cells with more than 14 stations to all stations is believed to be related to the expected increase in variation due to decreasing sample size.

The areal extent of the anomalous regions rarely reached the areal extent of the medium-size anomalies shown in Figures 8–10. Three separate Monte Carlo realizations were combined to simulate the stacking of methane, ethane, and propane into a composite map. As expected, the stacking process reduced the random anomalies. In no cases were any of these stacked random anomalies even close to the size and strength of the three largest anomalies observed in the survey data. Most were the size of the smaller survey anomalies. The stacking of methane, ethane, and propane anomalies strongly supports the conclusion that the large/strong anomalies result from subsurface hydrocarbon seepage, not from random data fluctuations.

The Monte Carlo simulations pointed out the importance to this technique of maintaining a relatively constant sampling density. Many of the small consistent anomalies were located in areas where the cells had few stations (edges, holes, sparse sampling), introducing a spatial bias to the cell procedure. The size of this spatial biasing is proportional to the sparseness of the data in the cell. This is in agreement with the increased range of expected fractions (p) for a binomial distribution as the number of samples decreases. This is easily seen for a cell with only one station; it is either 100% above or below the population median. This does not mean that several contiguous anomalous cells with few samples should be ignored. Rather, it means that these cells are ambiguous. The cells suggest anomalous leakage, but more samples in the area would be needed before the fractions from the cells can be trusted.

In this example, we chose the median value of the population as our definition of high and low magnitude seepage, resulting in a binomial distribution

Table 2. Cells with Fractions Above Survey Median Magnitudes (greater than 0.82 and 0.76, and less than 0.24 and 0.18) for Methane, Ethane, and Propane*

	>0.82	>0.76	<0.24	<0.18
Cells With More Than 14 Stations				
Methane	4%	10%	9%	6%
Ethane	4%	8%	7%	3%
Propane	2%	6%	7%	3%
All Cells				
Methane	6%	12%	14%	11%
Ethane	7%	11%	13%	9%
Propane	6%	10%	14%	10%

*There are 604 cells with more than 14 stations in them and a total of 1248 cells in the survey area. Totally random data would have approximately 0.5% of the cells above 0.82 and 2.5% above 0.76 for a sample size of 18. Note the higher percentages if all cells are counted, due to the presence of cells with 14 or fewer stations in them, pointing out the importance of trying to maintain a constant sampling density.

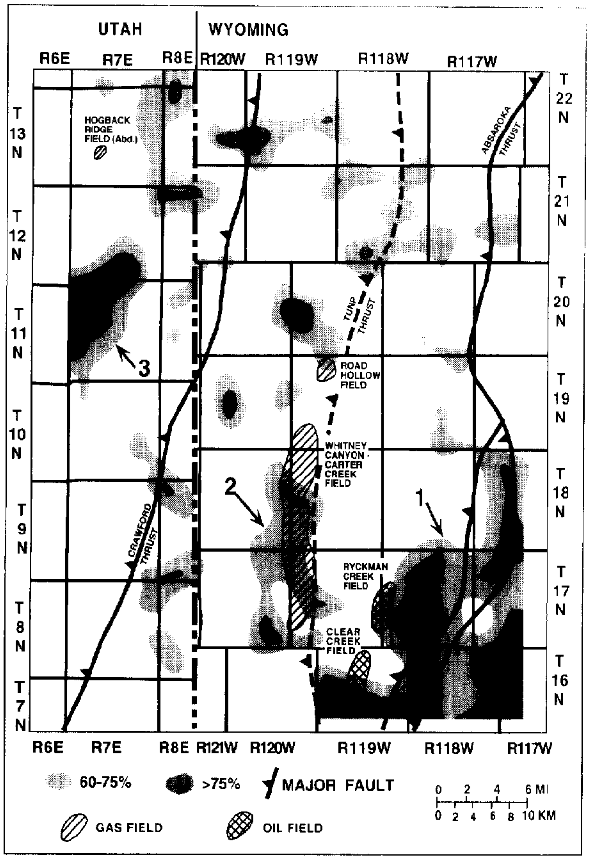

Figure 12—Composite gas map of the study area, showing selected fields and significant faults. This map shows the composite (methane, ethane, and propane) areas with high proportions of samples above the median of each respective hydrocarbon concentrations. The three major hydrocarbon anomalies are designated by the large numbers 1, 2, and 3. See the text for a detailed description of these anomalies.

with population (P) equal to 0.5. We could, however, have selected any other value, such as a higher magnitude, which would have resulted in a binomial distribution with a different P and correspondingly different confidence limits.

INTERPRETATION

The stacking of methane, ethane, and propane fractions (Figure 11) into a composite gas map (Figure 12) provides the most stable presentation of regional hydrocarbon seepage.

An indication of the expected composition of the migrating hydrocarbons (oil, condensate, gas, or a mixture) can be estimated by examining some of the ratios between methane, ethane, and propane. An empirically determined range of microseep ratio data is shown in Table 3. Note that these boundaries are not exact. The compositional ratios in Table 3 can be used as a standard to compare with the ratios of the anomalies associated with the known fields shown in Table 4.

The three anomalies with the largest fractions and covering the largest area will be examined in detail, moving from the east to the west (Figure 12). Anomaly 1 is in Wyoming T16N, R117-119W; T17N, R117-118W; and T18N, R117W. Anomaly 2 is in Wyoming T17N, R119-R120W, and T18N, R119-120W. Anomaly 3 is in Utah T11N, R7E, and T12N, R7E.

Anomaly 1 is the single largest, strongest (highest fraction of values above the median), and most continuous anomaly within the study area. It is located in the southeastern part of the survey area in the vicinity of the Clear Creek and Ryckman Creek fields (Figure 12). Anomaly 1 is supported by methane, ethane, and propane. The center of this anomaly is located to the east (updip) of Ryckman Creek field. The southwestern limit of this anomaly is located over a large part of Clear Creek field. This anomaly is in the region where the surface trace of the Absaroka fault splits into two major segments. The fracturing associated with these fault segments appears to provide an excellent route for migrating hydrocarbons.

Anomaly 2 does not cover as large an area or have percentages as high as Anomaly 1 on the composite gas map (Figure 12) because of the smaller frequency of above-median ethane and propane values. This anomaly is in the vicinity of Whitney Canyon-Carter Creek field. A number of localized faults that are exposed at the surface over the field apparently allows this anomaly to be more vertically associated with the field.

A more exact comparison may be made by comparing the surface seep ratios and the ratios obtained directly from the produced gases of the fields given in Table 5.

The surface composition information for both anomalies indicates that the subsurface accumulations should be either condensate with gas or gas and oil with some dry gas. Furthermore, the C_2/C_3 ratio implies that hydrocarbons in any fields around anomaly 2 (near Whitney Canyon-Carter Creek

Table 3. Approximate Range of Microseep Compositional Ratios for Dry Gas, Gas and Condensate (or Gas and Oil), and Oil*

	C_3/C_1 (× 1000)	C_2/C_3 (× 10)
Dry Gas	2-20	25-50
Gas and Condensate (or Oil)	20-60	16.5-25
Oil	60-500	10-16.7

*Adapted from Jones and Drozd (1983). These numbers can be used to predict the probable hydrocarbon composition at depth.

Table 4. Average Microseep Composition Ratios Over the Three Main Productive Fields in the Study Area*

Field	Anomaly**	C_3/C_1 (× 1000)	C_2/C_3 (× 10)
Ryckman Creek	1	20	20
Clear Creek	1	10–15	20
Whitney Canyon–Carter Creek	2	15–30	15–50

*Compare these numbers to those in Table 3.
**Anomaly numbers refer to specific areas of Figure 12.

field) may be somewhat drier than trapped hydrocarbons around anomaly 1 (near Ryckman Creek and Clear Creek fields), which is the actual situation.

The C_2/C_3 values for both of the anomalies and their underlying fields are in general agreement with respect to trend and amount. The C_3/C_1 surface sample values for anomaly 2, associated with Whitney Canyon–Carter Creek field, are in agreement with the range of values obtained from the produced gases. The C_3/C_1 values for anomaly 1 (associated with Ryckman Creek and Clear Creek fields) are, however, richer in C_1 than the produced gases. This suggests that there are biogenic or higher maturity hydrocarbon source rocks that have added methane to the surface seeps. Deeper or shallow sources of methane may have different migrating pathways than the Lower Cretaceous source rock that have sourced the existing fields.

Anomaly 3 is on the Crawford thrust sheet. Valenti (1987) documented that there are Lower Cretaceous source rocks under the Crawford thrust that should have generated significant quantities of hydrocarbons. He theorized that the hydrocarbons were never trapped and were dispersed along the migration pathways or at the surface. The hydrocarbons in anomaly 3 are probably being sourced from Lower Cretaceous source rocks under the Crawford thrust sheet, as predicted by Valenti. The C_3/C_1 values for this anomaly range between 0.015 and 0.025, indicating a gas and condensate composition (see Table 2). The C_2/C_3 values vary between 2.0 and 2.5, also within the gas and condensate range. The exploration challenge in this case is to explore for traps in the area of the anomaly that have the reservoir, cap rock, and geometry necessary to contain economic quantities of hydrocarbons.

As shown by these anomalies, the composition ratios are not exact tools for predicting the composition of the hydrocarbons at depth. However, they are very useful as general compositional tools and should be used as such. Interpretation of ratio data is also made more complex when multiple sources occur vertically in the same area. In those cases, the ratios are a weighted average of the subsurface variation where the weighting factors are unknown. We believe that the mixing of hydrocarbons at depth is controlled by the pressure associated with each subsurface hydrocarbon mass and by the ease of its communication to the surface.

RESULTS

The technical success of our study can best be judged by comparing the hydrocarbon magnitudes and compositions of the samples with appropriate yardsticks. Two yardsticks exist: (1) location and composition of known fields within the area, and (2) location and maturity of known source rocks in the area.

The first yardstick is strictly applicable only in the region of known production. There are two productive trends within the study area: (1) eastern, containing Clear Creek and Ryckman Creek fields (condensate and gas), and (2) western, containing Whitney Canyon–Carter Creek field (gas and some condensate).

With respect to soil-gas magnitude, as expressed by regions of above-average concentrations of hydrocarbons, the two trends were identified. The interpretation technique used in this study highlighted large areas that overlay or are near the major known fields. An exact overlay was not expected because of significant regional dip in the study area, variable pathways to the surface, and the processing techniques employed.

Comparison of the composition of the hydrocarbons in the reservoirs with the composition predicted by the light hydrocarbon ratios is quite close. Only the Ryckman Creek and Clear Creek fields' C_3/C_1 value predicted a significantly different composition than is present. This ratio suggests the existence of an independent methane source in this area. However, the overall production trend from condensate and gas in the east to more gas in the west is also found in the compositional ratios in the microseep samples.

The association of the anomalies with surface traces of faults supports the hypothesis that preferential permeability pathways are important factors

Table 5. General Composition Ratios of Produced Hydrocarbons from the Three Main Fields in the Study Area*

Field	C_3/C_1 (× 1000)	C_2/C_3 (× 10)
Ryckman Creek	66–67	20–21
Clear Creek	59	23
Whitney Canyon–Carter Creek	24–35	26–41

*Compare these numbers to those in Table 3.

controlling the surface location of hydrocarbon seepage. The lack of anomalies along other fault segments supports the hypothesis that there must be pressurized subsurface source of hydrocarbons, in addition to a preferential permeability pathway.

CONCLUSIONS

Regional cell maps were made for methane, ethane, and propane values in the study area. These maps were based on the fraction of samples within a 9-mi^2 area that were above the survey median for that particular gas component. The fractions from the three gases were then combined to create the composite map. The composite map allows a more regional view of the samples and a statistical test of the significance of anomalies on the individual gas maps. Microseep surveys that have been processed in this manner will supply the explorationist with a helpful regional tool that has a significantly different perspective than traditional exploration tools. Care must be exercised to assure that anomalies related to under sampled areas (edges, holes, etc.) are not over interpreted.

REFERENCES CITED

Davis, J. C., 1973, Statistics and data analysis in geology: New York, John Wiley and Sons, p. 381-389.

Dixon, J. S., 1982, Regional structural synthesis, Wyoming salient of Western thrust belt: AAPG Bulletin, v. 66, p. 1560-1580.

Dixon, W. J., and F. J. Massey, Jr., 1957, Introduction to statistical analysis, New York, McGraw-Hill, 488 p.

Jones, V. T., and R. J. Drozd, 1983, Prediction of oil or gas potential by near-surface geochemistry: AAPG Bulletin, v. 67, p. 932-952.

Lamerson, P. R., 1982, The Fossil basin area and its relationship to the Absaroka thrust system, *in* R. B. Powers, ed., Geologic studies of the Cordilleran thrust belt: Rocky Mountain Association of Geologist, v. 8, p. 279-340.

Link, W. K., 1952, Significance of oil and gas seeps in world oil exploration: AAPG Bulletin. v. 36, p. 1505-1541.

Matthews, M. D., V. T. Jones, and D. M. Richers, 1984, Remote sensing and hydrocarbon leakage: Proceedings of the 3rd International Symposium on Remote Sensing of the Environment, p. 663-670.

Peterson, J. A., 1973, Paleozoic shelf margins, northern Rocky Mountains: Geological Society of America Abstracts with Programs, v. 5, no. 3, p. 501.

Peterson, J. A., 1977, Paleozoic shelf-margins and marginal basins, western Rocky Mountains-Great Basin, United States, *in* E. L. Heisey, D. E. Lawson, eds., Rocky Mountain thrust belt geology and resources: Joint Wyoming-Montana-Utah Geological Associations Guidebook, p. 135-154.

Peterson, J. A., 1980, Depositional history and petroleum geology of the Permian Phosphoria, Park City, and Shedhorn formations, Wyoming and southeastern Idaho: U. S. Geological Survey Open-File Report 80-667, 42 p.

Petroleum Information Corporation, 1981, The thrust belt–1981: Denver, Colorado, Petroleum Information Corporation, 251 p.

Petroleum Information Corporation, 1991, Wyoming oil and gas production report: Denver, Colorado, Petroleum Information Corporation, 51 p.

Pratch, J.-C., 1985, Oil and gas accumulations in thrust belts: Journal of Petroleum Geology, v. 8, p. 129-148, 297-322.

Royse, F., Jr., M. A. Warner, and D. L. Reese, 1975, Thrust belt structural geometry and related stratigraphic problems, Wyoming, Idaho and northern Utah, *in* D. W. Bolyard, ed., Symposium on deep drilling frontiers in the central Rocky Mountains: Rocky Mountain Association of Geologist, p. 41-54.

Sieverding, J. L., and F. Royse, Jr., 1990, Whitney Canyon-Carter Creek field–U.S.A.: western Wyoming thrust belt, *in* E. A. Beaumont and N. H. Foster, compilers, Structural traps III: tectonic fold and fault traps: AAPG Treatise of petroleum Geology Atlas of Oil and Gas Fields, p. 1-29.

Valenti, G. L., 1987, Review of the hydrocarbon potential of the Crawford thrust plate Wyoming-Idaho-Utah thrust belt: *in* W. R. Miller, ed., Wyoming Geological Association Guidebook, p. 257-266.

Walker, J. D., 1982, Hogback Ridge field, Rich County, Utah: thrust-belt anomaly or harbinger of future discoveries?, *in* R. B. Powers, ed., Geologic studies of the Cordilleran thrust belt: Rocky Mountain Association of Geologist, v.2, p. 581-590.

Warner, M. A., 1982, Source and time of generation of hydrocarbons in the Fossil basin, western Wyoming thrust belt, *in* R. B. Powers, ed., Geologic studies of the Cordilleran thrust belt. Rocky Mountain Association of Geologist, v. 2, p. 805-815.

ABOUT THE AUTHORS

ROGER G. DICKINSON

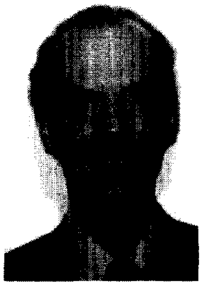

Roger G. Dickinson graduated from the University of Oregon in 1972 with an M.S. degree in geology. Since graduation, he has worked as a petroleum geologist with Texaco. His current work is concentrated in southern Wyoming and northwest Colorado. Geological and geochemical assignments with Texaco have been in California, Alaska, throughout the Rocky Mountain region, and select areas of Nevada, Texas, and Kansas.

MARTIN D. MATTHEWS

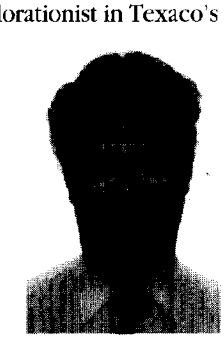

Matt Matthews is a consulting explorationist in Texaco's Frontier Exploration Department. Prior to this, he was a senior scientist with Texaco's Exploration and Production Technology Department, held a variety of positions with Gulf Research and Development Company (including manager of geochemical research and director of geological research), was a senior staff geologist for Gulf Oil U.S., and was assistant professor of geology at Washington State University. He received his B.S. degree from Allegheny College (1960), his M.S. degree from West Virginia University (1963), and his Ph.D. from Northwestern University (1973).